Fast electron density methods in the life sciences—a routine application in the future?

Peter Luger*

Received 24th April 2007
First published as an Advance Article on the web 15th June 2007
DOI: 10.1039/b706235d

The understanding of mutual recognition of biologically interacting systems on an atomic scale is of paramount importance in the life sciences. Electron density distributions that can be obtained from a high resolution X-ray diffraction experiment can provide—in addition to steric information—electronic properties of the species involved in these interactions. In recent years experimental ED methods have seen several favourable developments towards successful application in the life sciences. Experimental and methodological advances have made possible on the one hand high-speed X-ray diffraction experiments, and have allowed on the other hand the quantitative derivation of bonding, non-bonding and atomic electronic properties. This has made the investigation of a large number of molecules possible, and moreover, molecules with 200 or more atoms can be subject of experimental ED studies, as has been demonstrated by the example of vitamin B_{12}. Supported by the experimentally verified transferability concept of submolecular electronic properties, a key issue in Bader's *The Quantum Theory of Atoms in Molecules*, activities have emerged to establish databases for the additive generation of electron densities of macromolecules from submolecular building blocks. It follows that the major aims of any experimental electron density work in the life sciences, namely the generation of electronic information for a series of molecules in a reasonable time and the study of biological macromolecules (proteins, polynucleotides), are within reach in the near future.

Introduction

X-Rays interact with the electron distribution of a chemical structure and give a discrete diffraction pattern in the case of a periodic arrangement as present in crystals. It follows that the results from an X-ray diffraction experiment contain information about the electron density distribution $\rho(\boldsymbol{r})$ in a crystal,[1] so that this quantity is a physical observable in contrast, for example, to the wave functions in the Schrödinger equation. It should, however, be mentioned that conventional X-ray analysis, which is nowadays carried out worldwide several tens of thousands of times per year, only yields atomic positions and some information about their vibrational behaviour, since the method is based on the independent atom model (IAM) formalism, which considers spherical electron densities (EDs) only, so that all aspherical ED deformations caused by bonding and non-bonding interactions are *a priori* neglected.

Institute for Chemistry and Biochemistry/Crystallography, Free University of Berlin, Fabeckstr. 36a, 14 195, Berlin, Germany. E-mail: luger@chemie.fu-berlin.de

Peter Luger obtained a degree in mathematics and physics in 1968, and then directed his interest to crystallography, which led to the award of a Ph.D. in 1970. Since 1979 he has been a Professor of Crystallography at the Freie Universität Berlin, Germany. His main interest is experimental structure research, with a special focus on electron density studies.

Peter Luger

Aspherical EDs are commonly described by a more complicated model introduced by Hansen and Coppens (1978),[2] generally referred to as the multipole model, where an aspherical ED of an atom is given by

$$\rho_a(\boldsymbol{r}) = \rho_{core}(r) + P_v\kappa^3\rho_{val}(\kappa r) + \rho_{def}(\boldsymbol{r}) \quad (1)$$

with

$$\rho_{def}(\boldsymbol{r}) = \sum_{l=0}^{l_{max}} \kappa'^3 R_l(\kappa' \boldsymbol{r}) \sum_{m=-1}^{1} P_{lm} Y_{lm}(\theta, \phi)$$

While the first two terms still describe spherical core and valence densities, the third term is used to model aspherical density contributions.

As an alternative procedure to model aspherical EDs, the maximum entropy method (MEM) has been used in some cases. MEM tries to maximize an entropy function of a grid-based ED, starting from a given prior ED.[3] It has recently been applied in the bioorganic field, and the results were compared to multipole modelling.[4]

The substitution of the IAM by the aspherical model raises strict requirements for the X-ray diffraction experiment, making for decades the execution of experimental ED work possible only in exceptional cases. Thanks to the technical advances of the last few years, the situation has changed significantly, as will be detailed below.

The importance of the electron density $\rho(\boldsymbol{r})$ as a fundamental property of an electronic system follows from the Hohenberg–Kohn theorem[5] (the Nobel prize was awarded to Walter Kohn in 1998, together with John Pople). It states that the ground state energy of a non-degenerate quantum chemical system is functionally related to its distribution of charge. As a consequence, major electronic properties of bonding and non-bonding interactions, atomic properties, stability and reactivity can be deduced from the ED.

In the life sciences it is a fundamental challenge to understand the recognition and interaction of biologically active systems on an atomic scale. It is generally accepted that not only steric interactions but also complementary electronic properties of the involved species play a dominant role in this recognition process. Experimental electron density distributions contain, among other things, information on weak intermolecular interactions in the crystal. They can serve in a first approximation as a model for the interactions under biological conditions, since the same types of effects as the ligand–target interactions should exist in the crystal (*e.g.* steric, electrostatic, hydrogen bonding, van der Waals effects), and these are expected to be comparable in size. In this respect, experimental ED properties are much better suited to simulate physiological conditions than those from isolated molecule calculations, as has been shown in a number of studies.[6–8] For a broad application of experimental ED work in the life sciences, (at least) two major problems have to be addressed:

(i) Screening: in medicinal chemistry (drug development) it is indispensable to screen a large number of compounds to identify their potential activity. This makes also the generation of electronic information on series of molecules in short time periods necessary.

(ii) Macromolecules: proteins and polynucleotides are important biological macromolecules, but for several reasons (crystal quality, disorder problems, limited diffraction properties) ED studies on these types of molecules are known only in exceptional cases. Pioneering work in this field has been carried out in the group of Lecomte (Nancy, France).[9–12]

A reasonable application of experimental ED research in the life sciences therefore makes an approach to the above-mentioned problems necessary. It will be shown in this contribution that from the present status and extrapolation to the near future, this method has the power to become routinely used in this field.

The present state of electron density research

Experimental and methodological advances

The ED of a chemical structure consists of a large spherical and a very small aspherical contribution located mainly in the covalent bond and certain non-bonding (lone pair) regions. To make these small aspherical effects visible, very precise X-ray diffraction experiments have to be carried out requiring single crystals of excellent quality. Since thermal movement of atoms in the crystal lattice should be as small as possible, X-ray data collection should be performed at the lowest attainable temperature. Moreover, at low temperature, high-order data, which are needed not only to improve accuracy and resolution, but also to provide sufficient data for the refinement of the increased number of parameters of the multipole model (see eqn (1)), are more likely to have significant intensities above the background.

The above-mentioned experimental conditions were extremely difficult to meet until various technical advances in the last decade led to a major breakthrough in ED work:[13]

(i) The appearance of CCD area detectors in the mid-1990s increased the amount of X-ray data able to be collected in a given time by one or two orders of magnitude, compared to point detectors, leading to a drastic reduction of exposure time.

(ii) Highly intense synchrotron beamlines provided a bright source of X-ray radiation. The high primary intensity and the tuneable wavelength, allowing a choice of $\lambda \approx 0.5$ Å or shorter, enabled very high-resolution data sets to be collected.[14]

(iii) The introduction of open-flow or closed-cycle He cooling devices allowed ED X-ray data collection at extremely low temperatures (around 10–20 K).

Fig. 1 illustrates an example of a proper ED data set measured for the tripeptide L-alanyl-L-tyrosyl-L-alanine[15] under almost optimum experimental conditions.

A data set of more than 200 000 reflections was collected at a wavelength of 0.50 Å using open-flow He gas stream cooling, allowing measurement at 9 K. Although a resolution of $d = 0.40$ Å ($\sin\theta/\lambda = 1/2d = 1.24$ Å^{-1}) was reached, the number of reflections significantly above the background was greater than 90%. The static deformation density map in the plane of one peptide bond shows clearly the expected aspherical features in the covalent bonding and the non-bonding (lone pair) regions.

While the static map shown in Fig. 1 yields more or less qualitative (or at most semi quantitative) information, a variety of quantitative results is provided by Bader's *The Quantum Theory of Atoms in Molecules* (QTAIM).[16,17] Making use of the first and second partial derivatives of the electron density function $\rho(\boldsymbol{r})$, the electron density gradient vector field $\nabla\rho(\boldsymbol{r})$ and the corresponding Laplacian $\nabla^2\rho(\boldsymbol{r})$ are generated. A proper definition of atoms and bonds is then given and a topological analysis of $\rho(\boldsymbol{r})$ can be carried out, which allows a quantitative description of atoms, bonds, non-bonding interactions, electronic structure and reactivity. In this concept, a bond is defined by its bond path, a line of maximum ED in the gradient vector field. The value of the electron density $\rho(\boldsymbol{r}_{BCP})$ at a bond critical point $\boldsymbol{r}_{BCP}$ on the bond path (defined by the condition that $\nabla\rho(\boldsymbol{r})$ vanishes at $\boldsymbol{r}_{BCP}$) is then a quantitative measure for the strength of a bond.

Making use of the zero-flux surfaces in the ED gradient vector field $\nabla\rho(\boldsymbol{r})$, a well-defined procedure of partitioning a chemical structure into atomic regions is provided. Once the shape and the volume of an atom is known, a number of atomic or functional group properties can be evaluated; for instance, atomic charges can be obtained by integration over the charge density in the given atomic volume.

The above-mentioned experimental and methodological advances have been completed by the development and distribution of specific computer program systems (*e.g.* XD,[18] Valray,[19] Mopro[12,20]) providing algorithms for the refinement, analysis and visualization of experimental ED results.

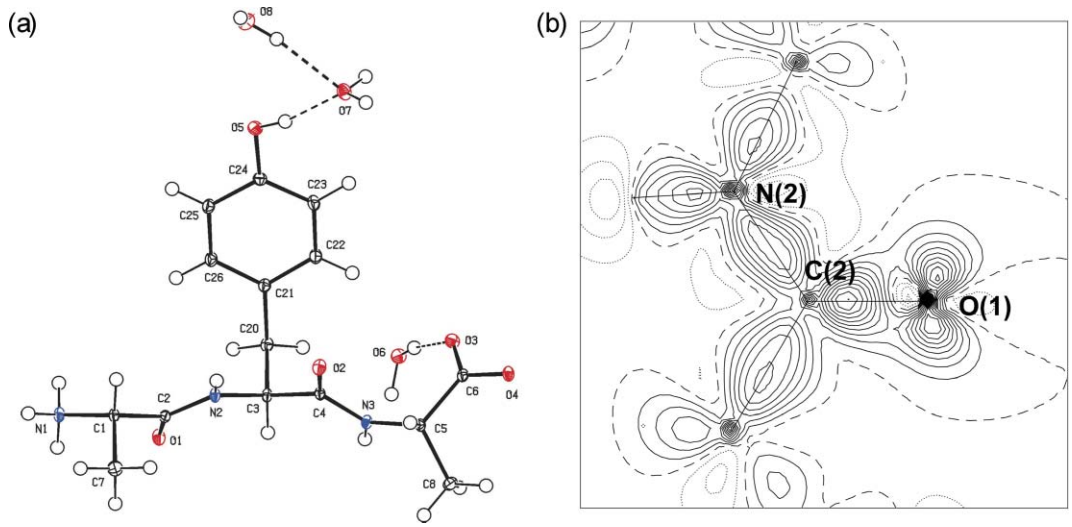

Fig. 1 a) Structure of the tripeptide L-alanyl-L-tyrosyl-L-alanine (water modification)[15] from a data set of 203 534 reflections measured at 9 K using open-flow He gas stream cooling (Helijet, Oxford Diffraction) at synchrotron beamline D3 (Hasylab/DESY, Hamburg, Germany), wavelength $\lambda =$ 0.50 Å, resolution $d = 0.40$ Å ($\sin\theta/\lambda = 1.24$ Å^{-1}), MAR165-CCD area detector. b) Static deformation density in the peptide bond region given by the plane through N2, C2, O1, positive/zero/negative contours as solid/dashed/dotted lines, contour intervals 0.1 e Å^{-3}.

Intermolecular interactions, hydrogen bonds

One of the greatest discoveries in the life sciences of the last century was the double helix structure of DNA introduced by Watson and Crick,[21] which could not have been developed unless the existence of hydrogen bonds between the base pairs was assumed. In almost all biological systems, hydrogen bonds and other weak interactions play an important role. Various approaches exist to analyze these interactions quantitatively and qualitatively in electron density distributions.

Koch and Popelier[22] have evaluated eight concerted effects occurring in the ED that are indicative of hydrogen bonding, while Espinosa *et al.*[23–25] have derived exponential relations for hydrogen bond energies from the analysis of experimental ED studies. These quantitative topological criteria allow a better insight into the strengths of these interactions than steric criteria being applied in geometry analysis programs.

A more qualitative description, making the site and direction of intermolecular interactions clearly visible, is illustrated in Fig. 2, in which two types of iso-surface representations are shown generated with the interactive graphics program Moliso,[26] written in our lab. Fig. 2a shows the molecular Hirshfeld surface[27,28] of the Watson–Crick base pair complex 9-methyladenine–1-methylthymine (A–T complex), in which the experimentally refined ED is mapped on the A and T surfaces. The intermolecular hydrogen bonds are shown by the strong-colored circular regions.

Fig. 2b shows the electrostatic potential of the nucleoside thymidine (derived from the experimental ED using the method of Su and Coppens[29]) mapped on the ED iso-surface at 0.5 e Å^{-3}. A pronounced polarization is visible, in that negative regions (in red) surround the electronegative oxygens, while a positive potential (in blue) surrounds the H atoms. The hydrogens, which are donor atoms in hydrogen bonds, exhibit the most strongly positive regions, as can be seen for the OH hydrogens H13 and H14 (in purple).

It follows that experimental ED distributions also provide qualitative and quantitative information on the weak intermolecular interactions that play an important role in biological recognition processes.

Recent applications—two examples

Protease inhibitor model compounds

In the course of the development of cysteine and aspartic protease inhibitors consisting of electrophilic building blocks that can covalently block the nucleophilic amino acids of the enzymes' active sites, the aziridine model compound **1** (Fig. 3) was synthesized.[30] This compound is known to undergo nucleophilic ring opening by cleavage of the C–C bond of the aziridine three-membered ring, and it was important to know at which of the two ring carbons the nucleophilic attack would occur.

An experimental ED study provided information on this question, as is illustrated in Fig. 4, which allows a close look at the situation in the reactive region of the three-membered ring. The electrostatic potential (Fig. 4a) obtained from the crystalline ED[29] shows that carbon atom C1 is much more positively polarized than C2, so that it will be the preferred site for a nucleophilic attack. The zero Laplacian iso-surface, also called the "reactive surface" after Bader,[16] shows the exact location of the electrophilic centres, represented by holes in this iso-surface, thus allowing additional insight into the direction of nucleophilic attack (Fig. 4b).

A comparison with model reactions with oxygen and sulfur nucleophiles revealed that the aziridine **1** reacts according to the electronic properties derived from the ED study, *i.e.* nucleophilic attack takes place exclusively at C1.

ED studies on vitamin B_{12}

As already mentioned, experimental ED studies become increasingly difficult with increasing molecular size. In this respect,

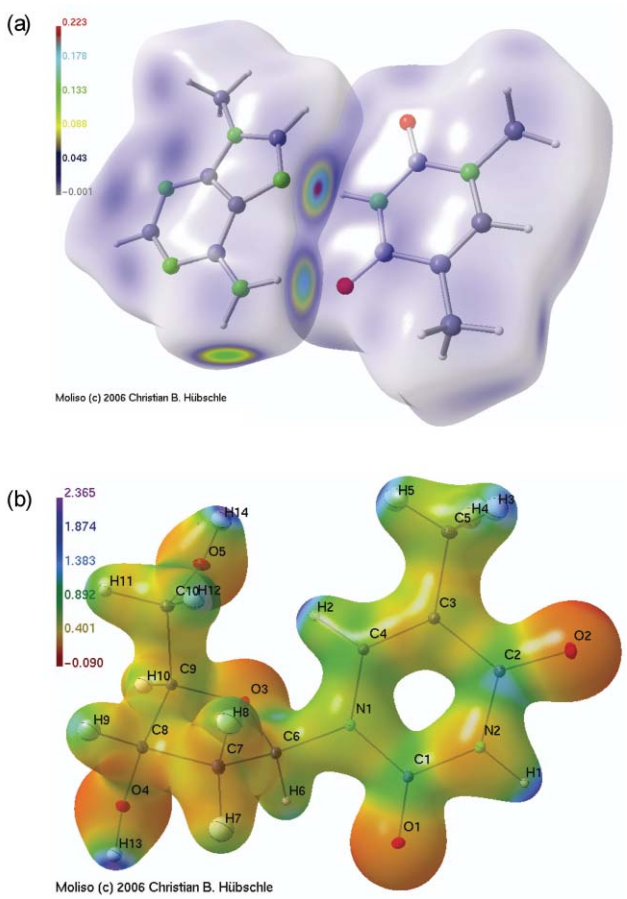

Fig. 2 (a) Hirshfeld surface of the Watson–Crick base pair complex 9-methyladenine–1-methylthymine, colour-mapped with the electron density. The three intermolecular hydrogen bonds are shown by the strong-colored circular regions. The colour legend refers to units of e Å^{-3}. (b) Molecular electrostatic potential of thymidine mapped on the charge density iso-surface at 0.5 e Å^{-3}. The colour legend refers to units of e Å^{-1}. MolIso representations[26] are used. Reproduced with permission from the International Union of Crystallography (Copyright 2006).

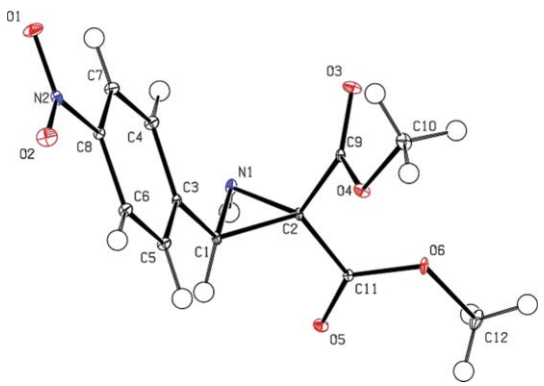

Fig. 3 ORTEP[63] representation with displacement ellipsoids at 9 K (50% probability) of the aziridine protease inhibitor model compound **1** with atom numbering scheme. Hydrogen atoms are represented by small spheres of arbitrary radius.[30] Reproduced with permission from Wiley-VCH (Copyright 2007).

vitamin B_{12} (cyanocobalamine, CN-Cbl), the corresponding coenzyme (5′-deoxy-5′-adenosylcobalamine, Ado-Cbl) and further

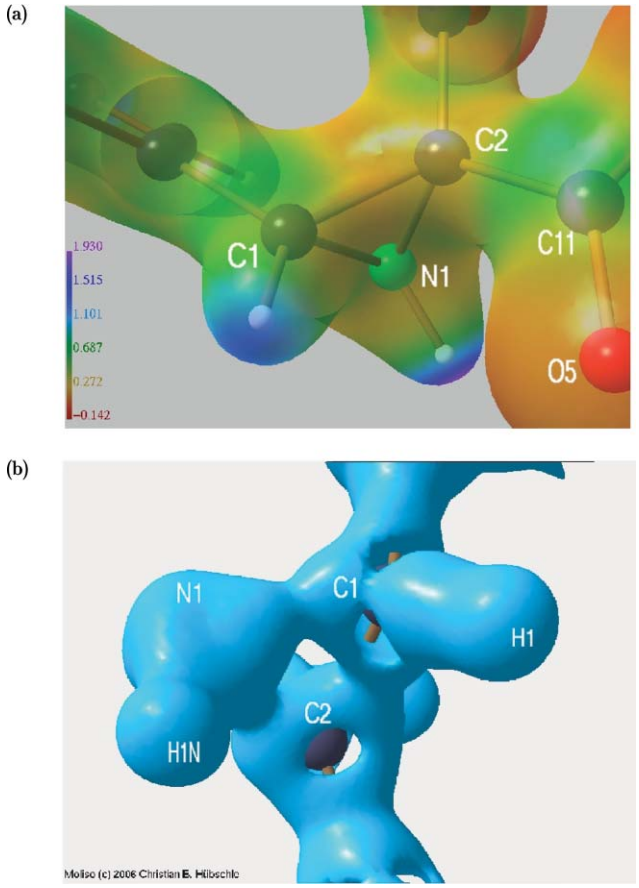

Fig. 4 (a) Experimental electrostatic potential mapped on an iso-surface of the density at 0.5 e Å^{-3} for the aziridine ring of **1**. Colour bar scale in e Å^{-3}. (b) Experimental zero Laplacian iso-surface of the three-membered ring region of aziridine **1**.[30] MolIso representations[26] are used. Reproduced with permission from Wiley-VCH (Copyright 2007).

related alkylcobalamines (R-Cbl), consisting of 200 or more atoms are borderline cases between small and macromolecular structures, and thus present a challenge for ED determination.

Alkylcobalamines play an important role in human metabolism. They are cofactors of mammalian enzymes that catalyze several biological processes, methyl transfer, isomerization and redox reactions. An important scientific aspect is the fact that the alkylcobalamines belong to the few biologically relevant compounds with metal–carbon bonds. Interestingly, this bond is stable under physiological conditions and in the presence of oxygen.[31] The participation of cobalt, which is the rarest of the first-row transition metal elements in the earth's crust and the oceans, suggests that special functionality is involved.

From the various reasons given above, an experimental ED study seemed of interest, especially with regard to the electronic structure of the corrin system, the electronic configuration of the Co centre and the nature of the Co–X bonds.

Although crystal structures of the alkylcobalamines have been described as notoriously inaccurate due to the disorder of side chains and solvent molecules,[32] crystals of a new solvate of vitamin B_{12} could be grown (with 12 water and 3 propanol molecules per B_{12} molecule in the asymmetric unit, of which only one propanol molecule was disordered) that were properly suited for high-resolution data collection. Based on more than 660 000

reflections collected at 100 K with conventional MoKα radiation to a resolution of $d = 0.41$ Å ($\sin\theta/\lambda = 1.22$ Å^{-1}), an experimental ED could be derived.[33] As an example, the experimental static deformation electron density distribution in the corrin ring is displayed in Fig. 5. As expected for an octahedral cobalt-ion coordination, a lock-and-key arrangement is clearly seen; regions of electron accumulation are concentrated on the lines bisecting the N–Co–N angles, while electron deficiency is located along the Co–N bonds. Topological analysis which gives ED values at the bond critical points indicates Co–X bonds of decreasing strength for the Co–CN, Co–N_{eq} and Co–N_{ax} bonds. For further details of the results, see ref. 33.

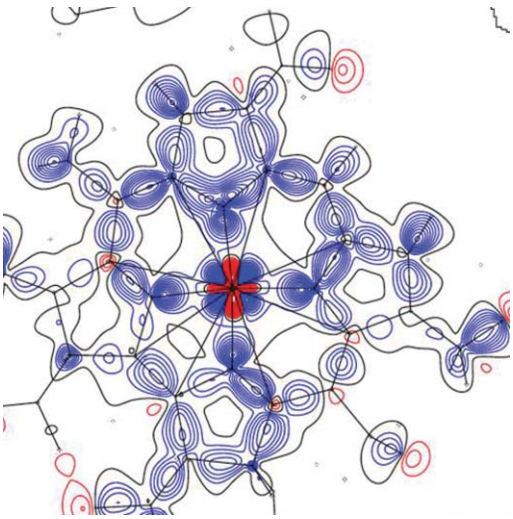

Fig. 5 Experimental static deformation electron density in the corrin ring of the vitamin B_{12} solvate. Positive, zero, and negative contour lines are in blue, black, and red; the contour interval is 0.1 e Å^{-3}.[33] Reproduced with permission from Wiley-VCH (Copyright 2007).

This study has shown that a conventional X-ray diffraction experiment can provide data of sufficient quality even for the ED determination of a large structure such as this vitamin B_{12} derivative, which contains more than 250 atoms in the asymmetric unit.

A similar investigation on the related coenzyme Ado-Cbl is in progress so that a comparison of results with respect to their different biological function will be possible.

Transferability of submolecular/atomic properties

As already mentioned, Bader's *The Quantum Theory of Atoms in Molecules*[16,17] provides a procedure to partition a molecular structure into submolecular regions, functional groups or single atoms making use of the zero-flux surface in the electron density gradient vector field $\nabla\rho(\boldsymbol{r})$. A key issue of Bader's theory is the transferability of submolecular properties. On the electronic level, it is expected that density and derived properties of a functional group composed of atomic fragments should possess a high degree of transferability when compared for different but chemically related molecules.

It follows that once the density properties of an atom or a group of atoms in a given chemical neighbourhood are known, the same properties should be assumed to exist if this atom occurs in another molecule but in the same chemical environment. The transferability of submolecular or atomic electronic properties provides a tool to use these fragments as building blocks for the additive generation of the electronic densities of macromolecules such as proteins or oligo/polynucleotides. Since the transferability concept is essential for the application of database approaches to the modelling of the EDs of larger systems, something which has recently become of vital interest to various groups,[34–37] an experimental verification was of major importance. The biologically important class of the twenty genetically encoded amino acids was the first one where this transferability was systematically examined from experimental and theoretical work. While Bader and Matta[38–40] have published complete topological data on all twenty amino acids based on theoretical calculations, experimental studies on sixteen of them were carried out by different groups.[41] This class of compounds is thus the first one for which a complete set of theoretical ED data is available and for which the corresponding experimental studies are approaching completeness.

It was shown that the bond topological properties ($\rho(\boldsymbol{r}_{BCP})$ values and corresponding Laplacians) of the five bonds common to all amino acids (C=O, C–O(H), C–N, C_α–C′ and C_α–C_β) agree within standard uncertainties of 0.07–0.11 e Å^{-3} and 2–5 e Å^{-5} for $\rho(\boldsymbol{r}_{BCP})$ and $\nabla^2\rho(\boldsymbol{r}_{BCP})$. Since comparable discrepancies were reported in the literature for averages from other experimental studies and also for the results obtained from different data sets of one compound,[42,43] the above-mentioned experimental results are very consistent in their respective ranges despite the various experimental conditions, different β-substituents and crystal environments.

An obvious step from single amino acids to polymeric structures is the consideration of oligopeptides containing the building blocks of proteins. Following this route, we have examined the transferability of bond topological properties, atomic volumes and charges in the peptide bond region of several oligopeptides.

Fig. 6 presents comparative considerations of bond topological properties ($\rho(\boldsymbol{r}_{BCP})$ and $\nabla^2\rho(\boldsymbol{r}_{BCP})$ values) in the main chain of six tripeptides of the type L-Ala-Xxx-L-Ala, with Xxx = L-alanine (A),[44] glycine (G),[45] L-histidine (H), L-proline (P)[46] and L-tyrosine (Y, two modifications, AYA·EtOH and AYA·H_2O[15]). Neglecting the influence of different next-nearest neighbours, the peptide groups next to the N-terminus and the C-terminus are considered to consist of bonds of the same type. Standard deviations (after averaging) of 0.06 e Å^{-3} and 2.9 e Å^{-5} are then obtained, confirming the results from the experimental amino acid study.

For comparing the transferability of atomic volumes and charges in the peptide bond region, we made use of experimental data for five dipeptides, one hexapeptide and four tripeptides of the above-mentioned L-Ala-Xxx-L-Ala type. The results obtained so far are summarized in Fig. 7.[47] The averages of comparable quantities show that the internal consistency for volumes is <1 Å^3. However, if the provision of equal nearest neighbours is no longer fulfilled, significant deviations from the overall averages can be recognized. This holds for the C_α atom of the glycine and the nitrogen atom of the proline residues. The average volumes of the (non-Gly) C_α atoms are smaller by more than 1 Å^3 than those of the Gly C_α atoms, where the second hydrogen atom allows the carbon to expand. A nearest neighbour influence is also seen for the N atoms. In proline the nitrogen atom is part of the five-membered

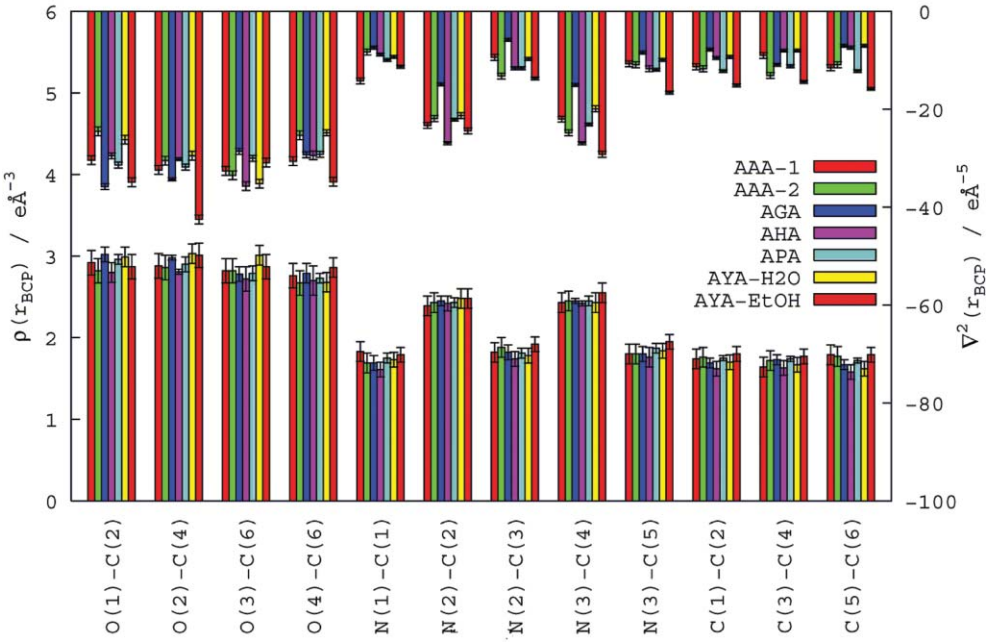

Fig. 6 Bond topological properties $\rho(\boldsymbol{r}_{BCP})$ (in e Å^{-3}) and $\nabla^2\rho(\boldsymbol{r}_{BCP})$ (in e Å^{-5}) in the main chain of six tripeptides.

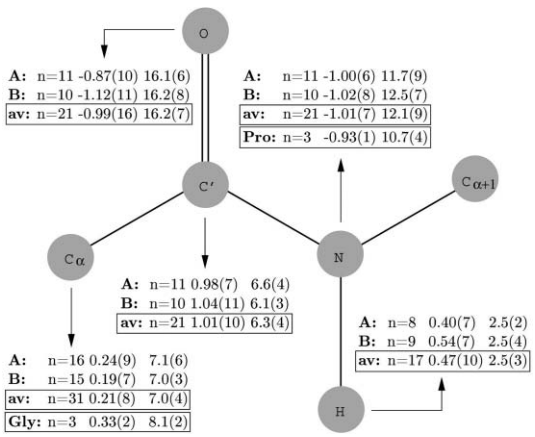

Fig. 7 Average atomic charges (in units of e) and volumes (in Å^3) of the atoms in the peptide bond region. **A** refers to five dipeptides and one hexapeptide; **B** refers to the four tripeptides AAA·$\frac{1}{2}$H$_2$O, APA·H$_2$O, AYA·C$_2$H$_5$OH; **av** is the average over all entries. *N* is the number of contributing entries.[47] Reproduced with permission from Wiley-VCH (Copyright 2007).

ring and bonded to a third carbon atom instead of hydrogen, which reduces the volume by more than 1 Å^3, analogous to the above-quoted volume expansion for the glycine C$_\alpha$.

The AIM charges (for averages see also Fig. 7) agree within the given atom types by 0.07–0.16 e. The C$_\alpha$ atoms carry a small positive charge, the hydrogens of the peptide NH group are moderately positively charged, and the C′ atoms carry a high positive charge, while strong negative charges close to 1 e are seen on the N and O atoms. The sum of the positive charges is approximately +1.7 e, while the negative charges amount to about −2 e, so that for each peptide bond region the excess of −0.3 e has to be compensated by the side chains.

A conclusion of these studies on amino acids and the peptide bonds of oligopeptides is that very reproducible atomic and bond topological properties for the contributing atoms can be derived when the chemical environments are comparable. No significant experimentally detectable influence of the next-nearest neighbours on the electron density of a given type of atom or bond was found. If there is any influence, it is beyond the accuracy of experimental ED work at present. These findings confirm experimentally the nearest/next-nearest neighbour approximation,[48] and encourage the use of the database approaches currently being developed for ED determinations of polypeptides or other macromolecules where the transferability principle is an essential prerequisite for their validity.

Perspectives

Fast data collection

It was mentioned in the introduction that one prerequisite for the successful application of experimental ED work in the life sciences is the execution of fast X-ray diffraction experiments to make a series of investigations possible. In other words, the use of high-throughput techniques (already established in several fields of X-ray diffraction based structure research, such as small-molecule and protein crystallography), would be highly desirable.

About a decade ago we reported on a high-resolution data collection experiment[49] combining synchrotron primary radiation and CCD area detection, carried out within one day, that could have otherwise taken weeks or even months. Now the experimental situation has further improved, in that a reduction of exposure time to hours or minutes seems to be within reach. This was recently demonstrated by a 12 hour sequence of diffraction experiments having been conducted at the synchrotron beamline X10SA of the Swiss Light Source (SLS) of the Paul Scherrer Institute (Villigen,

Switzerland).[50] In this time period a total of more than 400 000 reflections were collected for four data sets at a resolution of $d = 0.5$ Å ($\sin\theta/\lambda = 1.0$ Å^{-1}). Thanks to the brilliant primary intensity of this third generation synchrotron source, significant intensities could be obtained even for otherwise extremely small and weakly diffracting crystals in very high-order regions of reciprocal space.

In an additional very quick test experiment, a data set of 22 000 reflections for an adenosine crystal was collected in less than one hour, which was entered into an aspherical atom refinement. As a result, Fig. 8 shows the static deformation density map in the purine plane of the adenosine molecule. All the expected features in the bonding and non-bonding regions are resolved practically noise-free, despite being based on a data set with the shortest exposure time ever applied in experimental ED work.

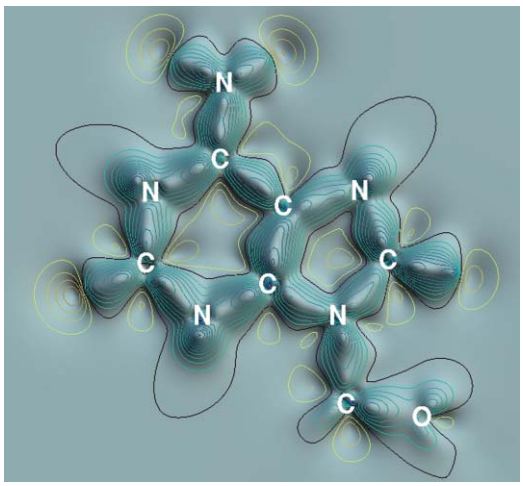

Fig. 8 Relief plot of the experimental static deformation density of the purine plane of adenosine based on a synchrotron data set collected at beamline X10SA (SLS, PSI) in less than one hour.[50] Reproduced with permission from the American Chemical Society (Copyright 2005).

To examine the possible shortcomings of high-speed data collections, we compared one of the four SLS data sets, taken for a crystal of the tripeptide L-Ala-Gly-L-Ala (hereafter called the SLS data set) with two further state-of-the-art data sets, one collected under home laboratory conditions (the Home data set), and the other using synchrotron radiation at the Hasylab/DESY facility in Hamburg, Germany (the Hasylab data set).[45]

As summarized in Table 1, the three data sets were measured under very different experimental conditions with respect to diffractometer setup, radiation type and wavelength, detector type, temperature and beam time period (which varied between 4 hours and more than 5 days).

The multipole refinement according to eqn (1) was carried out with exactly the same model in all three cases, so that the quantitative results are directly comparable. For the SLS data, collected in the shortest exposure time, the number of reflections and the resolution were the lowest, which might have negatively influenced the results, however, this could not be confirmed. Fig. 9 shows the values of the ED at the BCPs and the corresponding Laplacians for the 14 non-H bonds. For each bond, averages of the three experimental contributions and the corresponding ESDs, σ_n, were calculated. Averaging over the 14 σ_n values gave mean uncertainties of 0.07 e Å^{-3} and 3.4 e Å^{-5} for the densities and Laplacians, respectively. For atomic volumes and charges, average uncertainties were found to be 0.4 Å^3 and 0.1 e. Since all of these uncertainties are in the same range, as have been reported in the literature for the accuracy of these topological descriptors, it follows that in no case can an indication for a preference of any of the three data sets be derived.

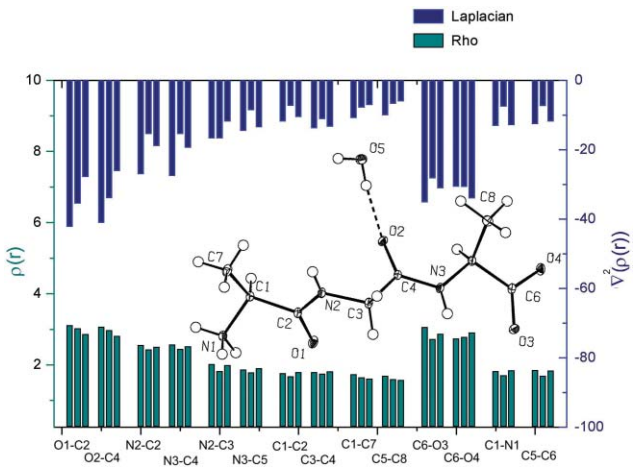

Fig. 9 Bond topological properties $\rho(\boldsymbol{r}_{BCP})$ (in e Å^{-3}) and $\nabla^2\rho(\boldsymbol{r}_{BCP})$ (in e Å^{-5}) of the tripeptide L-alanyl-glycyl-L-alanine obtained from three data sets. Representation in three columns for each bond. First column: home data set; second column: SLS data set; third column: Hasylab data set.[45]

Considering also the result of the 1 hour experiment of adenosine (Fig. 8), the expectation that high-speed ED experiments with exposure times of hours or minutes should be routine in the near future seems justified. This is further supported by recent reports

Table 1 Experimental conditions for three data collections of L-Ala-Gly-L-Ala

	Home	Hasylab	SLS
Beamline	Huber (home)	F1	X10SA
Detector	APEX	MARCCD-165	MAR-CCD-225
Cooling system	He-cryostat	N_2-flow	N_2-flow
Temperature/K	20	100	92
Radiation type	MoKα	Synchrotron	Synchrotron
Wavelength/Å	0.7107	0.55	0.6214
Exposure time/h	130	28	4
Max. resolution in d/Å	0.42	0.40	0.51
Max. resolution in $(\sin\theta/\lambda)$/Å^{-1}	1.18	1.25	0.98
Total no. of reflections	32 605	97 469	28 133
R/R_w (multipole)	0.036/0.023	0.026/0.022	0.027/0.039

on extremely sensitive detectors that should allow the collection of entire data sets in time periods of a few seconds.[51,52]

However, the present shortcomings of the experimental situation should not be overlooked. Most synchrotron beamlines are dedicated to protein crystallography, where high-order regions of reciprocal space do not need to be explored and where hard X-rays (say $\lambda < 1$ Å) cannot be used, because from the large unit cell dimensions an overlap of neighbouring reflections would occur. These problems are mainly of a geometric nature and could be overcome with little effort, especially in the course of designing new beamlines. The development of the small molecule beamline I19 at DIAMOND (Oxford, UK; to start operation in 2008) deserves in this respect the attention of the ED experimenter community.

Database developments: invariomsA

A further highly desirable application of ED in the life sciences would be on macromolecules, *e.g.* proteins, but unfortunately this is generally not practicable. One reason stems from the poor diffraction properties of protein crystals, and another from a drawback of the multipole formalism, in that the number of parameters becomes very large with increasing molecular size, causing (among other things), correlation and convergence problems.

Bader's concept of transferability of submolecular electronic properties, which has been verified experimentally as outlined above, opens the possibility of establishing databases of atomic building blocks for the additive generation of the EDs of larger molecules. This would help to limit the number of parameters, even for macromolecules, and there is considerable current research activity in this field. A database of experimentally determined multipole parameters from X-ray data of high quality was established in the group of Lecomte (Nancy, France).[35,36] Applications were reported for a few protein data sets, for which, as rare exceptions, high resolutions of $d < 1.0$ Å could be obtained. For example, studies on crambin (resolution $d = 0.54$ Å)[10] and the scorpion toxin II ($d = 0.96$ Å)[11] were published in 2000, and more recently the same group reported on an ongoing study of aldose reductase ($d =$ 0.66 Å),[12,53] for which the starting values from their experimental database were used for the protein ED refinement.

A theoretical data bank, in which parameters were averaged over a selection of related organic compounds, was developed in the group of Coppens (Buffalo, US).[37]

We have introduced recently a database of so-called invariomsA,[34] also based on theoretical calculations, in which each entry is derived from a unique model compound. This concept and a few applications will be described here briefly.

Invariomsa (from invariant atoms) are intermolecular transfer-invariant pseudoatoms within the Hansen–Coppens formalism (eqn (1)). They allow the generation of individual aspherical scattering factors that take into account the chemical neighbourhood of a bonded atom. In this way the spherical independent-atom model (IAM) can be replaced. The procedure to establish an invariom database, which relies—like all other database approaches—on the electron density transferability principle, works as follows:[54]

An invariom is assigned to a given bonded atom by a model compound consisting of the same elements and the same local chemical environment. This includes nearest neighbours for single-bonded systems, and next-nearest neighbours for delocalized/mesomeric systems, H atoms and hypervalent elements.

After geometry optimization of the model compound by a quantum chemical calculation, theoretical structure factors are generated in a simulated periodic environment (cubic cell, space group $P\bar{1}$), which are then used to obtain invariom scattering factors from a multipole refinement of the simulated data with the corresponding least-squares program XDLSM of the XD suite.[18]

After completion, for each atom in a given chemical environment, a set of aspherical multipole parameters is obtained, which can be stored in an invariom library. The total density of a molecule is obtained by superposition of its constituting invariomsa. Fig. 10 shows as an example the molecular structure of serine, with an atom numbering scheme, invariom names (which follow a simple notation; see ref. 34 and 55 for details) and corresponding model compounds.

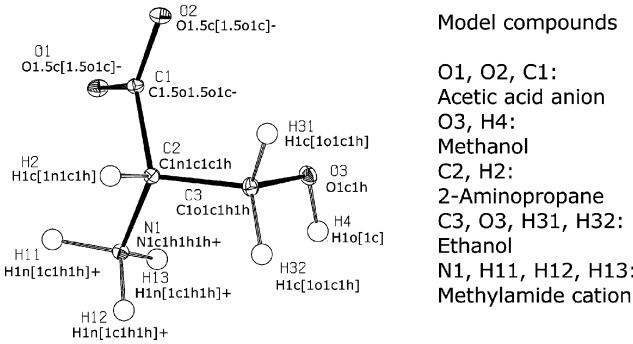

Fig. 10 ORTEP plot[63] of the molecular structure of DL-serine at 20 K with atom numbering scheme, assigned invariomsa and the model compounds used to obtain the invariom electron density.[47] Reproduced with permission from Wiley-VCH (Copyright 2007).

The modelling procedure of an invariom refinement, where only positional and displacement parameters are adjusted against the experimental intensities, can be automated, helping to expedite this otherwise time-consuming procedure significantly. For this purpose, the program INVARIOMTOOL has been developed[56] which automatically analyses molecular geometry, assigns invariom names to each atom in a given structure, uses this invariom name to find and transfer the corresponding density parameters of the data bank, and writes input files for the respective aspherical-atom refinement program part of XD.[18] In addition, the local site symmetry and coordinate system for each atom is selected and included. Once high-resolution ED quality data for a 'classical' multipole refinement are available, INVARIOMTOOL can also be applied to generate the starting model, which requires appreciable effort, if made individually.

Until now, all of the 20 naturally occurring amino acids were analyzed in terms of their invariom fragments, resulting in a database with 73 entries generated from 37 model compounds,[54] completely covering this class of compounds. Comparable work is in progress to establish invariomsa in the nucleoside/nucleotide field, so that two important macromolecular classes, proteins and oligo/polynucleotides, can be the subject of invariom applications.

Two examples should illustrate some qualitative and quantitative results of invariom applications.

A couple of years ago, the ED of the pharmacologically active compound terbogrel was investigated by Flaig *et al.*[6] The experimental ED for this molecule, consisting of more than

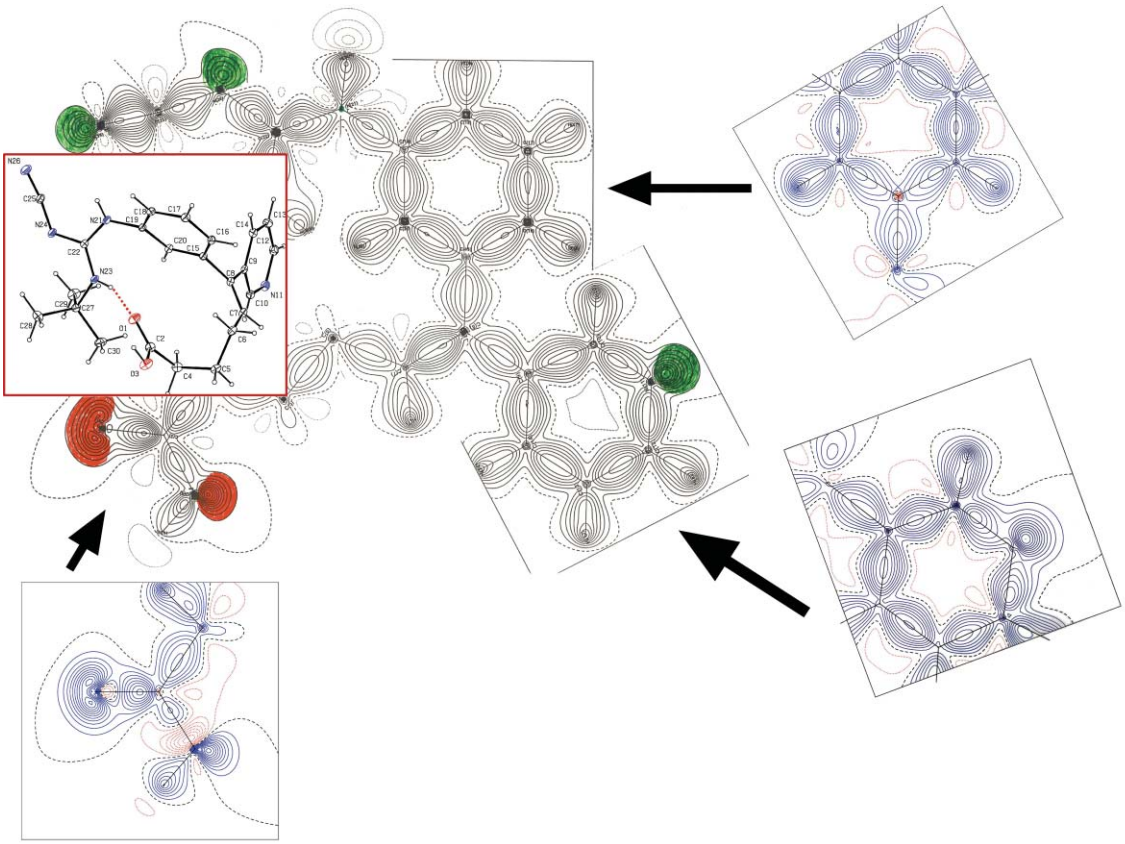

Fig. 11 Large map: experimental static deformation electron density of terbogrel based on 220 000 high-resolution reflections, $d = 0.4$ Å (inset: molecular structure). Small maps: corresponding static maps in the planes of the phenyl ring, pyridine ring and carboxyl group after invariom application on a data set of 3300 reflections measured at room temperature (resolution $d = 0.86$ Å). Contour interval is 0.1 e Å^{-3}.

50 atoms, was derived from a data set of about 220 000 reflections measured at 100 K to a resolution of 0.4 Å ($\sin\theta/\lambda = 1.25$ Å^{-1}). These data were the subject of a 'classical' multipole refinement to yield, among other results, the static deformation density map shown in Fig. 11. Based on a second data set of 3300 reflections measured at room temperature at a much lower resolution of $d = 0.86$ Å ($\sin\theta/\lambda = 0.58$ Å^{-1}), invariom application yielded static maps of comparable quality (see Fig. 11). The electrostatic potential obtained from invariom modelling of the low-resolution data (Fig. 12) shows in detail the expected charge distribution on the various functional side groups of this molecule.

Quantitative implications from applying invariom can be drawn from the example of the tripeptide L-Ala-L-Pro-L-Ala,[46] for which three models were considered: a 'classical' multipole model ('ref') based on a 0.37 Å resolution data set of more than 180 000 reflections measured at 100 K, an invariom model applied to the same fully resolved data set ('inv0.37') and an application of the invariom formalism where the data set was cut to the low resolution limit of $d = 0.83$ Å ('inv0.83'). As illustrated in Fig. 13, there is practically no difference between the results from the two invariom models despite the different resolutions, showing clearly the ability to successfully apply the invariom formalism to data sets that just satisfy the minimum resolution requirements of commonly used data sets for spherical structure determination. The average agreement with the results from a full multipole

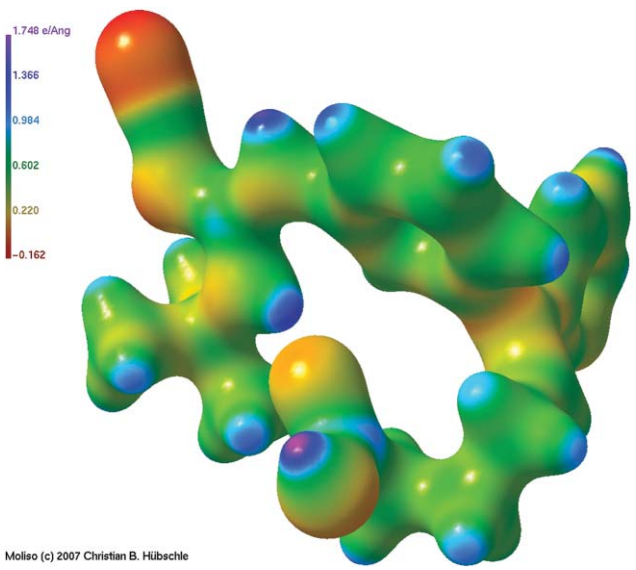

Fig. 12 Electrostatic potential mapped on the ED iso-surface at 0.5 e Å^{-3} for terbogrel obtained from invariom application on the low-order data set (MolIso representation).[26]

refinement was derived to be within 0.08 e Å^3 and 1.0 e Å^{-5} for the electron density values and corresponding Laplacians at the bond

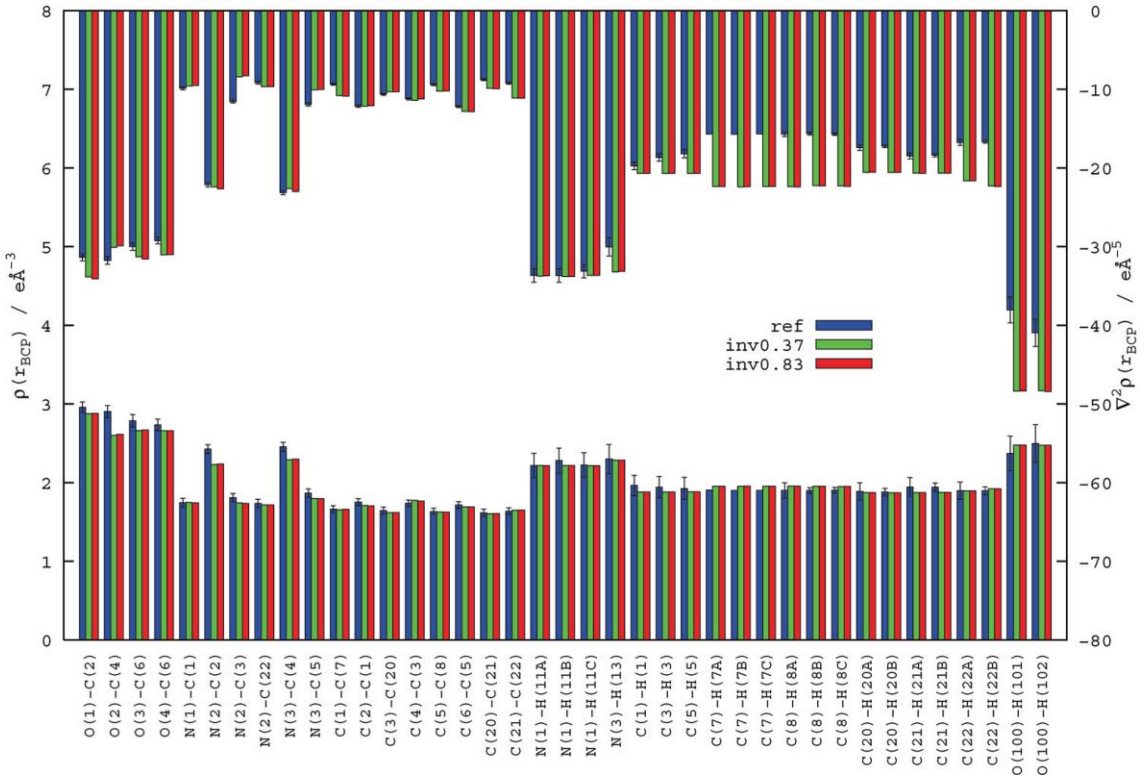

Fig. 13 Comparison of the classical multipole model (ref) with the two invariom models (inv0.37 and inv0.83) for L-alanyl-L-prolyl-L-alanine with respect to the bond topological properties $\rho(\boldsymbol{r}_{BCP})$ (in e Å^{-3}) and $\nabla^2\rho(\boldsymbol{r}_{BCP})$ (in e Å^{-5}).[46] Reproduced with permission from the International Union of Crystallography (Copyright 2007).

critical points, and 0.63 Å^3/0.09 e for Bader atoms/charges, in all cases clearly within the uncertainty ranges repeatedly quoted in the previous sections.

In a series of papers, Dittrich *et al.*[34,54–58] have explored various aspects of invariom applications, in which they addressed, among other things, questions such as invariom nomenclature,[34,55] invariom application on data sets at different temperature and resolution,[55] treatment of anomalous dispersion within the invariom formalism and consequences for reliable absolute structure assignment[57] and the validation of the invariom library on an extensive number of amino acids and peptide structures from the crystallographic literature.[54]

Whether or not transferability might be affected by strong intramolecular interactions due to protein secondary structures (*e.g.* β-sheets, α-helices) is very open at the moment, but it is an important issue to be examined further, something which should be feasible if more database studies of larger molecules are carried out.

From the present status of database developments and from our experiences with the invariom formalism, it can be concluded that for standard small-molecule structures, a rapid and easy-to-use procedure now exists that improves the structure refinement even for low-resolution data to yield ED distributions of an accuracy not far from that derived from multipole refinement on high-resolution data. Thanks to the strongly reduced experimental effort and the highly automated invariom application procedure, high-throughput techniques can be applied also in experimental ED work.

In protein crystallography, it can be expected that the number of available data sets measured at subatomic resolution will increase, given current developments in high intensity beamlines and detector technology. As invariom modelling should make use of data at a resolution of $d \leq 0.9$ Å (or $\sin\theta/\lambda > 0.55$ Å^{-1}), broad application is in sight.

Conclusions and outlook

It can be summarized that experimental ED methods have experienced several favourable developments in recent years for a successful application in the life sciences. Experimental and methodological advances have made possible on the one hand high-resolution X-ray diffraction experiments at an increased pace, and allowed on the other hand the derivation of reproducible and reliable results to describe bonding, non-bonding and atomic electronic properties quantitatively. Newer developments are devoted to the analysis of further local quantities such as the source function,[59,60] which analyses the contribution of various sources to the ED at a given point (*e.g.* a critical point), or the electron localization function (ELF), which identifies local electron concentrations.[61,62]

The transferability of submolecular/atomic electronic properties, a key issue of Bader's QTAIM, has been verified experimentally and has initated various activities for the introduction of databases aimed at replacing the independent atom model by a library consisting of more complex aspherical scattering factors.

It has been noted already that the aim of any experimental electron density research work in the life sciences should be directed to the investigation of series of molecules in a reasonable time and to the study of macromolecules (*e.g.* proteins) as a routine application. We believe that we have demonstrated that this aim has, in certain parts, either been reached, or will be reached in the near future.

Experimental ED work can be considered as a routine application if the following three tasks can be carried out with reasonable effort and in an acceptable time scale:

Task 1: High-order data collection, if required, for several hundred thousand reflections, and 'classical' multipole refinement to yield accurate quantitative ED properties. The provision is high intense primary radiation (at a synchrotron source), fast and sensitive area detection, and the help of INVARIOMTOOL software for a convenient multipole model assignment.

Task 2: Derivation of ED-quality properties from low-resolution X-ray data. The provision is the application of the invariom formalism.

Tasks 1 and 2 will allow high-speed ED studies of a series of molecules to meet the demand in medicinal chemistry to screen a large number of compounds.

Task 3: ED-studies of biological macromolecules. The provision is the collection of atomic-resolution X-ray data from 3rd-generation synchrotron beamlines and invariom application.

Since all of the above-mentioned provisions can be anticipated to be satisfied in the near future, experimental ED work will surely be applied routinely in the life sciences, so that the answer to the question raised in the title of this article will be "yes".

Acknowledgements

This work was financially supported by the Deutsche Forschungsgemeinschaft (DFG) in the framework of the SPP1178 (grant Lu 222/29-1/2). The assistance of Mrs M. Weber in preparing this manuscript is gratefully acknowledged. The author thanks also all co-workers and collegues who have provided various contributions to this article.

Notes and references

1 T. S. Koritsánszky and P. Coppens, *Chem. Rev.*, 2001, **101**, 1583–1627.
2 N. K. Hansen and P. Coppens, *Acta Crystallogr., Sect. A: Fundam. Crystallogr.*, 1978, **34**, 909–921.
3 S. van Smaalen, L. Palatinus and M. Schneider, *Acta Crystallogr., Sect. A: Fundam. Crystallogr.*, 2003, **59**, 459–469.
4 A. Hofmann, J. Netzel and S. van Smaalen, *Acta Crystallogr., Sect. B: Struct. Sci.*, 2007, **63**, 285–295.
5 P. Hohenberg and W. Kohn, *Phys. Rev. B: Solid State*, 1964, **136**, 864.
6 R. Flaig, T. S. Koritsánszky, R. Soyka, L. Häming and P. Luger, *Angew. Chem., Int. Ed.*, 2001, **40**, 355–359.
7 D. E. Hibbs, C. J. Austin-Woods, J. A. Platts, J. Overgaard and P. Turner, *Chem. Eur. J.*, 2003, **9**, 1075–1083.
8 N. E. Ghermani, A. Spasojevic-de Bire, N. Bouhmaida, S. Ouharziune, J. Bouligand, A. Layre, R. Gref and P. Couvreur, *Pharm. Res.*, 2004, **21**, 598–607.
9 C. Jelsch, V. Pichon-Pesme, C. Lecomte and A. Aubry, *Acta Crystallogr., Sect. D: Biol. Crystallogr.*, 1998, **54**, 1306–1318.
10 C. Jelsch, M. M. Teeter, V. Lamzin, V. Pichon-Pesme, R. H. Blessing and C. Lecomte, *Proc. Natl. Acad. Sci. U. S. A.*, 2000, **97**, 3171–3176.
11 D. Housset, F. Benabicha, V. Pichon-Pesme, C. Jelsch, A. Maierhofer, S. David, J. C. Fontecilla-Camps and C. Lecomte, *Acta Crystallogr., Sect. D: Biol. Crystallogr.*, 2000, **56**, 151–160.
12 C. Jelsch, B. Guillot, A. Lagoutte and C. Lecomte, *J. Appl. Crystallogr.*, 2005, **38**, 38–54.
13 P. Coppens, *Angew. Chem.*, 2005, **117**, 6970–6972.
14 R. E. Cachau and A. D. Podjarny, *J. Mol. Recognit.*, 2005, **18**, 196–202.
15 L. Chechinska, S. Mebs, C. Hübschle, D. Förster, W. Morgenroth and P. Luger, *Org. Biomol. Chem.*, 2006, **4**, 3242–3251.
16 R. F. W. Bader, *Atoms in Molecules – A Quantum Theory*, Clarendon Press, Oxford, UK, 1990 and 1994.
17 *The Quantum Theory of Atoms in Molecules*, ed. C. F. Matta and R. J. Boyd, Wiley-VCH, Weinheim, Germany, 2007.
18 T. Koritsánszky, S. T. Howard, T. Richter, P. Macchi, A. Volkov, C. Gatti, P. R. Mallinson, L. J. Farrugia, Z. Su and N. K. Hansen, *XD – A Computer Program Package for Multipole Refinement and Topological Analysis of Electron Charge Densities from Diffraction Data (Users Manual)*, Middle Tennessee State University (TN, USA); University of Milano (Italy); University at Buffalo (NY, USA); CNR-ISTM (Milano, Italy); University of Glasgow (UK), 2003.
19 R. F. Stewart, M. A. Spackman and C. Flensburg, *VALRAY98 (Users Manual)*, Carnigan Mellon University (Pittsburgh, PA, USA); University of Copenhagen (Denmark), 1998.
20 B. Guillot, V. L. Guillot, C. Lecomte and C. Jelsch, *J. Appl. Crystallogr.*, 2001, **34**, 214–223.
21 J. D. Watson and F. H. C. Crick, *Nature*, 1953, **171**, 737–738.
22 U. Koch and P. L. A. Popelier, *J. Phys. Chem.*, 1995, **99**, 9747–9754.
23 E. Espinosa, E. Molins and C. Lecomte, *Chem. Phys. Lett.*, 1998, **285**, 170–173.
24 E. Espinosa, M. Souhassou, H. Lachekar and C. Lecomte, *Acta Crystallogr., Sect. B: Struct. Sci.*, 1999, **55**, 563–572.
25 E. Espinosa, C. Lecomte and E. Molins, *Chem. Phys. Lett.*, 1999, **300**, 745–748.
26 C. B. Hübschle and P. Luger, *J. Appl. Crystallogr.*, 2006, **39**, 901–904.
27 M. A. Spackman and P. G. Byrom, *Chem. Phys. Lett.*, 1997, **267**, 215–220.
28 J. J. McKinnon, A. S. Mitchell and M. A. Spackman, *Chem. Eur. J.*, 1998, **4**, 2136–2141.
29 Z. Su and P. Coppens, *Acta Crystallogr., Sect. A: Fundam. Crystallogr.*, 1992, **48**, 188–197.
30 S. Grabowsky, T. Pfeuffer, L. Chechinska, M. Weber, W. Morgenroth, P. Luger and T. Schirmeister, *Eur. J. Org. Chem.*, 2007, 2759–2768.
31 *B12*, ed. D. Dolphin, Wiley, New York, 1982.
32 C. Kratky and B. Kräutler, *Chemistry and Biochemistry of B_{12}*, Wiley, New York, 1999.
33 B. Dittrich, T. Koritsánszky, A. Volkov, S. Mebs and P. Luger, *Angew. Chem., Int. Ed.*, 2007, **46**, 2935–2938.
34 B. Dittrich, T. Koritsánszky and P. Luger, *Angew. Chem., Int. Ed.*, 2004, **43**, 2718–2721.
35 V. Pichon-Pesme, C. Jelsch, B. Guillot and C. Lecomte, *Acta Crystallogr., Sect. A: Fundam. Crystallogr.*, 2004, **60**, 204–208.
36 V. Pichon-Pesme, C. Lecomte and H. Lachekar, *J. Phys. Chem. B*, 1995, **99**, 6242–6250.
37 A. Volkov, X. Li, T. Koritsánszky and P. Coppens, *J. Phys. Chem. A*, 2004, **108**, 4283–4300.
38 C. F. Matta and R. F. W. Bader, *Proteins: Struct., Funct., Genet.*, 2000, **40**, 310–329.
39 C. F. Matta and R. F. W. Bader, *Proteins: Struct., Funct., Genet.*, 2002, **48**, 519–538.
40 C. F. Matta and R. F. W. Bader, *Proteins: Struct., Funct., Genet.*, 2003, **52**, 360–399.
41 S. Mebs, M. Messerschmidt and P. Luger, *Zeitschr. f. Kristallogr.*, 2006, **221**, 656–664.
42 B. Dittrich, T. Koritsánszky, M. Grosche, W. Scherer, R. Flaig, A. Wagner, H.-G. Krane, H. Kessler, C. Riemer, A. M. M. Schreurs and P. Luger, *Acta Crystallogr., Sect. B: Struct. Sci.*, 2002, **58**, 721–727.
43 M. Messerschmidt, S. Scheins and P. Luger, *Acta Crystallogr., Sect. B: Struct. Sci.*, 2005, **61**, 115–121.
44 E. Rödel, M. Messerschmidt, B. Dittrich and P. Luger, *Org. Biomol. Chem.*, 2006, **4**, 475–481.
45 D. Förster, A. Wagner, C. B. Hübschle, C. Paulmann and P. Luger, *Z. Naturforsch., B: Chem. Sci.*, 2007, **62**, 696–704.
46 R. Kalinowski, *Diploma Thesis*, FU Berlin, 2006.
47 B. Dittrich and P. Luger, in: *The Quantum Theory of Atoms in Molecules*, ed. C. F.Matta and R. J. Boyd, Wiley-VCH, Weinheim, Germany, 2007, ch. 12.
48 T. Koritsánszky, A. Volkov and P. Coppens, *Acta Crystallog., Sect. A: Fundam. Crystallogr.*, 2002, **58**, 464–472.

49 T. Koritsánszky, R. Flaig, D. Zobel, H.-G. Krane, W. Morgenroth and P. Luger, *Science*, 1998, **279**, 356–664.
50 P. Luger, A. Wagner, Ch. B. Hübschle and S. I. Troyanov, *J. Phys. Chem. A*, 2005, **109**, 10177–10179.
51 Ch. Broennimann, E. F. Eikenberry, B. Heinrich, R. Horisberger, G. Huelsen, E. Pohl, B. Smitt, C. Schulze-Briese, M. Suzuki, T. Tomizaki, H. Toyokawa and A. Wagner, *J. Synchrotron Radiat.*, 2006, **13**, 120–130.
52 K. Hirano, T. Miyoshi, N. Igarashi, T. Takeda, J. Wu, T-t. Lwin, M. Kubota, N. Egami, K. Tanioka, T. Kawai and S. Wakatsuki, *Phys. Med. Biol.*, 2007, **52**, 2545–2552.
53 N. Muzet, B. Guillot, C. Jelsch, E. Howard and C. Lecomte, *Proc. Natl. Acad. Sci. U. S. A.*, 2003, **100**, 8742–8747.
54 B. Dittrich, C. B. Hübschle, P. Luger and M. A. Spackman, *Acta Crystallogr., Sect. D: Biol. Crystallogr.*, 2006, **62**, 1325–1335.
55 B. Dittrich, C. B. Hübschle, M. Messerschmidt, R. Kalinowski, D. Girnt and P. Luger, *Acta Crystallogr., Sect. A: Fundam. Crystallogr.*, 2005, **61**, 314–320.
56 C. B. Hübschle, P. Luger and B. Dittrich, *J. Appl. Crystallogr.*, 2007, **40**, 623–627.
57 B. Dittrich, M. Strümpel, T. Koritsánszky, M. Schäfer and M. A. Spackman, *Acta Crystallogr., Sect. A: Fundam. Crystallogr.*, 2006, **62**, 217–223.
58 R. Kingsford-Adaboh, B. Dittrich, C. B. Hübschle, W. S. K. Gbewonyo, H. Okamoto, M. Kimura and H. Ishida, *Acta Crystallogr., Sect. B: Struct. Sci.*, 2006, **62**, 843–849.
59 R. F. W. Bader and C. Gatti, *Chem. Phys. Lett.*, 1998, **287**, 133–238.
60 C. Gatti, F. Cargnoni and L. Bertini, *J. Comput. Chem.*, 2003, **24**, 422–436.
61 A. D. Becke and K. E. Edgecombe, *J. Chem. Phys.*, 1990, **92**, 5397–5403.
62 B. Silvi and A. Savin, *Nature*, 1994, **371**, 683–686.
63 M. N. Burnett and C. K. Johnson, *ORTEP-III: Oak Ridge Thermal Ellipsoid Plot Program for Crystal Structure Illustrations*, Report ORNL-6895, Oak Ridge National Laboratory, Oak Ridge, TN, USA, 1996.

